



Controlled oligomerization of [1.1.1]propellane through radical polarity matching: selective synthesis of SF₅- and CF₃SF₄-containing [2]staffanes

Jón Atiba Buldt[†], Wang-Yeuk Kong[†], Yannick Kraemer, Masiel M. Belsuzarri,
Ansh Hiten Patel, James C. Fettinger, Dean J. Tantillo^{*} and Cody Ross Pitts^{*}

Full Research Paper

Open Access

Address:

Department of Chemistry, University of California, Davis, 1 Shields Avenue, Davis, CA 95616, U.S.A.

Beilstein J. Org. Chem. 2024, 20, 3134–3143.

<https://doi.org/10.3762/bjoc.20.259>

Email:

Dean J. Tantillo^{*} - djtantillo@ucdavis.edu; Cody Ross Pitts^{*} - crpitts@ucdavis.edu

Received: 11 July 2024

Accepted: 06 November 2024

Published: 29 November 2024

* Corresponding author ‡ Equal contributors

This article is part of the thematic issue "Organofluorine chemistry VI" and is dedicated to Professor Josef Michl who recently passed away.

Keywords:

pentafluorosulfanylation; [1.1.1]propellane; radical chain oligomerization; staffanes; strain-release

Guest Editor: D. O'Hagan



© 2024 Buldt et al.; licensee Beilstein-Institut.
License and terms: see end of document.

Abstract

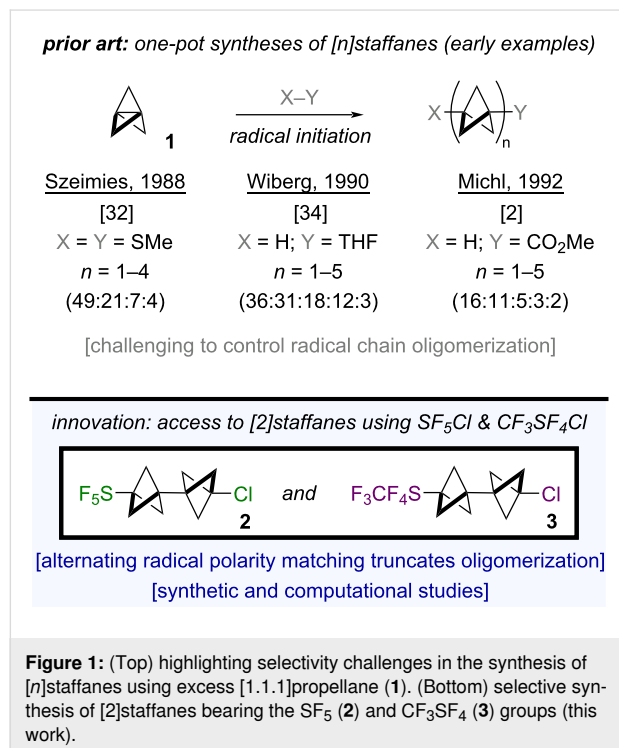
Selectivity in radical chain oligomerizations involving [1.1.1]propellane – i.e., to make $[n]$ staffanes – has been notoriously challenging to control when $n > 1$ is desired. Herein, we report selective syntheses of SF₅- and CF₃SF₄-containing [2]staffanes from SF₅Cl and CF₃SF₄Cl, demonstrating cases whereby oligomerization is preferentially truncated after incorporation of two bicyclopentane (BCP) units. Synthetic and computational studies suggest this phenomenon can be attributed to alternating radical polarity matching. In addition, single-crystal X-ray diffraction (SC-XRD) data reveal structurally interesting features of the CF₃SF₄-containing [2]staffane in the solid state.

Introduction

In various radical additions of X–Y across [1.1.1]propellane (**1**), functionalized oligomers known as $[n]$ staffanes – with $n > 1$, where n denotes the number of individual [1.1.1]bicyclopentane (BCP) linkers – are often observed and swiftly devalorized as *side-products* [1]. However, targeted synthesis of functionalized $[n]$ staffanes as rigid "molecular spacers" as proposed by Kaszynski and Michl [2–4] could facilitate new developments in

nanotechnology [5], liquid crystal design [6–10], and the study of energy-transfer [11,12] or electron-transfer [13–17] processes. We also posit that lower-order $[n]$ staffanes (i.e., $n = 2$ or 3) are potentially valuable C(sp³)-rich bioisosteres [18,19] that have been seemingly overlooked in the medicinal chemistry arena, in stark contrast to single BCP units over the past 12 years [20–24].

One plausible explanation for the paucity of applications of $[n]$ staffanes in materials or biological settings is a synthetic accessibility issue. For instance, dimerization of substituted BCPs [25–27] or photochemical appendage of **1** onto an extant BCP [28–31] are relatively effective tactics for the selective assembly of certain $[n]$ staffanes; the main caveat is that multiple synthetic steps are required. On the other hand, while a one-pot radical chain oligomerization is conceptually appealing, radical additions of X–Y across **1** in practice can be challenging to control and often lead to complex mixtures of functionalized $[n]$ staffanes, $n = 1–5$ (Figure 1, top) [2,31–34]. Even though $[n]$ staffanes are often separable by column chromatography, the yields for a single oligomer across a panoply of different transformations typically range from <1% to ≈30% when $n > 1$ is desired [35]. To the best of our knowledge, the assembly of functionalized $[n]$ staffanes from **1** in high yield/selectivity and in one step via controlled radical oligomerization remains a synthetic challenge.



Herein, we report proof-of-concept that our previous work on strain-release pentafluorosulfanylation of **1** [36] using SF_5Cl (prepared in house [37] under mild oxidative fluorination conditions [38–44]) can be extended to the selective synthesis of the associated chloropentafluorosulfanylated [2]staffane ($\text{SF}_5\text{-BCP-BCP-Cl}$, **2**), based on alternating radical polarity matching in the chain-propagation steps (Figure 1, bottom) [45–47]. Density functional theory (DFT) calculations provide insight into our observed selectivity, and our hypothesis is bolstered by computa-

tation of relative bicyclopentyl radical philicities. In addition, we demonstrate that similar reaction conditions can be applied to the synthesis of the analogous CF_3SF_4 -containing [2]staffane ($\text{CF}_3\text{SF}_4\text{-BCP-BCP-Cl}$, **3**). Finally, we examined compound **3** by SC-XRD and found that it undergoes a phase transition as a function of rate of cooling; this highlights that the [2]staffanes synthesized during this study are also interesting from a fundamental structural standpoint.

Results and Discussion

Over the past few years, our group has begun to establish strain-release pentafluorosulfanylation as a viable strategy for $\text{C}(\text{sp}^3)\text{-SF}_5$ bond formation [35,48]. For instance, in 2022, we reported a method for chloropentafluorosulfanylation of [1.1.1]propellane, i.e., to make $\text{SF}_5\text{-BCP-Cl}$ (**4**), that ostensibly proceeds through a radical chain propagation mechanism [36]. Under optimized conditions, we obtained product **4** in 86% yield, and the corresponding [2]staffane – $\text{SF}_5\text{-BCP-BCP-Cl}$ (**2**) – was formed as a minor side-product in 7% yield. While our original goal was to suppress formation of **2**, we later pondered whether preferential synthesis of compound **2** would also be possible. Accordingly, we began our screening process by systematically increasing the equivalents of [1.1.1]propellane (**1**) relative to SF_5Cl and evaluating the impact on selectivity (Table 1).

Table 1: Effect of [1.1.1]propellane (**1**) equivalents relative to SF_5Cl on selectivity^a.

	1	SF_5Cl <i>n</i> -pentane/Et ₂ O rt, 3 h	4	2	4:2
entry	1 (equiv)		4 (% yield) ^b	2 (% yield) ^b	
1	1.0		49%	4%	12:1.0
2	2.0		74%	22%	3.4:1.0
3	3.0		44%	29%	1.5:1.0
4	4.0		54%	40%	1.3:1.0
5	6.0		48%	45%	1.1:1.0
6	8.0		43%	53%	1.0:1.3
7	10		32%	51%	1.0:1.6
8	20		24%	72%	1.0:3.0
9 ^c	6.0		30%	63% (51%)^d	1.0:2.1

^aA 0.1 M solution of SF_5Cl in *n*-pentane (0.1 mmol) was added to a 0.8 M solution of [1.1.1]propellane in Et₂O under Ar atmosphere and stirred at rt for 3 h. ^bYield determined by ¹⁹F NMR; ^c SF_5Cl was added portion-wise. ^dIsolated yield.

A 0.1 M solution of SF_5Cl in *n*-pentane was added to a 0.8 M solution of **1** in Et₂O at room temperature, and the mixture was stirred for 3 hours prior to ¹⁹F NMR analysis. Upon increasing

from 1.0 to 6.0 equiv of **1**, we observed the **4:2** product ratio decreased dramatically from 12:1 to 1.1:1. Using 8.0 equiv of **1**, the ratio flipped such that **2** became the major product (i.e., **4:2** = 1:1.3) and was formed in 53% yield. Interestingly, even with 8.0 equiv of **1**, 96% of the material balance could be accounted for in the formation of *these two products alone* by ^{19}F NMR. To the best of our knowledge, this is an exceptionally rare instance whereby oligomerization of **1** appears to be stunted beyond formation of the [2]staffane; only trace yields of putative higher-order staffanes ($n > 2$) were detected in the crude reaction mixture. Remarkably, using 20 equiv of **1**, the observed **4:2** product ratio improved to 1:3, with **2** formed in 72% yield. In an even more extreme case, the [2]staffane still remained the major product formed in 66% yield when using 50 equiv of **1** (^{19}F NMR signals of presumed higher-order staffanes became more apparent, though their combined yield still remained \approx 18%).

Ultimately, we found adding SF_5Cl portion-wise – to keep the “effective” equiv of **1** higher at any given moment – proved to be a suitable compromise to access **2** in 63% yield by ^{19}F NMR (51% isolated) using 6.0 equiv of **1** (Table 1). We also demonstrated that this procedure can be performed on a 4.0 mmol scale (with respect to SF_5Cl) to provide access to \approx 0.5 g of **2** in

43% isolated yield. Additional details on reaction optimization can be found in Supporting Information File 1.

Upon increasing the equivalents of **1** during the screening process, we also found that irradiation with white LEDs was not necessary to boost product yields, as it was in our previously reported synthesis of **4** [36]. Both our laboratory [36] and the Qing laboratory [49] have previously observed that SF_5Cl additions to **1** can proceed in the absence of light. Note that recent work from the laboratories of Cahard and Bizet [50] suggests that autoxidation of the ethereal solvent could serve as one possible explanation for initial formation of SF_5 radicals in the absence of light to initiate a radical chain reaction. It is also well established that [1.1.1]propellane participates in radical-chain reactions (i.e., oligomerization) at room temperature in solution to form unsubstituted $[n]$ staffanes.

The origin of this innately controlled oligomerization was then investigated through density functional theory (DFT) calculations. The free energy profile of the radical chain propagation sequence was computed at the PWPPB95-D4/def2-QZVPP//PCM(Et_2O)- ω B97X-D/def2-TZVP level of theory [51–58] (Figure 2). Following addition of an SF_5 radical to **1** to form **INT1**, a Cl atom could be abstracted from SF_5Cl via **TS1** to

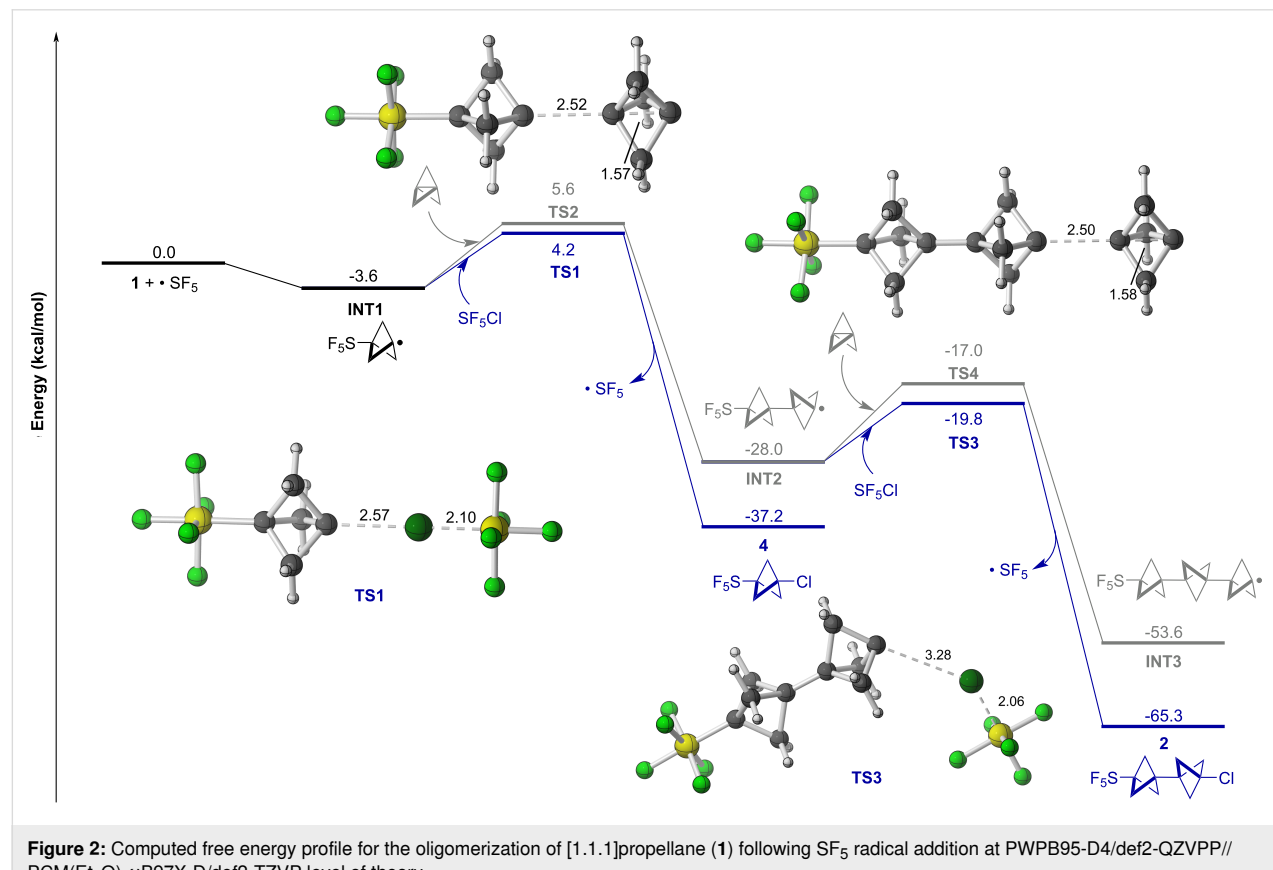


Figure 2: Computed free energy profile for the oligomerization of [1.1.1]propellane (**1**) following SF_5 radical addition at PWPPB95-D4/def2-QZVPP//PCM(Et_2O)- ω B97X-D/def2-TZVP level of theory.

form **4** or, alternatively, **INT1** could be added to another equiv of **1** via **TS2** to form **INT2**. Although formation of **4** is notably more thermodynamically favorable than **INT2** ($\Delta\Delta G = -9.2$ kcal/mol), a small difference in activation free energy is predicted ($\Delta\Delta G^\ddagger = -1.4$ kcal/mol). This, at least in part, provides an explanation as to how favoring the path to **INT2** may be achieved in practice through increasing concentration of **1**.

Subsequently, **INT2** could abstract a Cl atom from SF_5Cl via **TS3** to form **2** or add to a third equiv of **1** through **TS4**, leading to **INT3**. Once again, Cl atom abstraction is thermodynamically ($\Delta\Delta G = -11.7$ kcal/mol) and kinetically ($\Delta\Delta G^\ddagger = -2.8$ kcal/mol) favored. However, the $\Delta\Delta G^\ddagger$ is notably greater in the second product-determining step than the first product-determining step, which is consistent with our experimental observation that **2** forms preferentially over further oligomerization.

For another point of comparison, we examined the reactivity of **1** with $\text{CF}_3\text{SF}_4\text{Cl}$. This reagent is known to behave comparably to SF_5Cl in radical chain reactions [17,59–61] and can also be prepared conveniently in house [62]. In an analogous equivalents screen, we found that the **5:3** product ratio shifts from 7.7:1 using 1.0 equiv of **1** to 1:2.1 using 20 equiv of **1** (Table 2). In the latter scenario, 96% of the material balance could be accounted for in the formation of **5** and **3**, indicating oligomerization is likewise stunted beyond incorporation of two BCP units. Also similar to pentafluorosulfanylation conditions, we found that adding $\text{CF}_3\text{SF}_4\text{Cl}$ portion-wise to 6.0 equiv of **1** enables access to **3** in 60% yield by ^{19}F NMR (53% isolated).

Interestingly, we observed that aryl- SF_4Cl compounds do not follow the same selectivity trend as SF_5Cl and $\text{CF}_3\text{SF}_4\text{Cl}$ additions, suggesting that the controlled oligomerization phenomenon is quite sensitive to changes in the fluorinated sulfur reagent scaffold (see Supporting Information File 1 for more details).

This second instance of controlled oligomerization of **1** using $\text{CF}_3\text{SF}_4\text{Cl}$ was also studied at the PWPB95-D4/def2-QZVPP//PCM(Et_2O)- ω B97X-D/def2-TZVP level of theory (Figure 3). Addition of a CF_3SF_4 radical to **1** affords **INT4**, which can either abstract a Cl atom from $\text{CF}_3\text{SF}_4\text{Cl}$ via **TS5** to make **5** or add to another equiv of **1** via **TS6** to access **INT5**. As anticipated, chlorination of the radical is thermodynamically favored over addition to **1** ($\Delta\Delta G = -10.7$ kcal/mol). It is also predicted here that the free energy of activation is lower for chlorination, albeit only by 0.4 kcal/mol. This is consistent with the notion that the kinetic preference can be overcome by increasing the concentration of **1** relative to $\text{CF}_3\text{SF}_4\text{Cl}$. In the second product-determining step, Cl atom abstraction by **INT5** via **TS7** to make **3** is kinetically favorable over addition of a third equiv of **1** via **TS8** to access **INT6**, although the preference is not as large as for formation of **2** ($\Delta\Delta G^\ddagger = -1.3$ kcal/mol).

Thus, the predicted trend for both SF_5Cl and $\text{CF}_3\text{SF}_4\text{Cl}$ additions across **1** indicates a stronger preference for Cl atom abstraction over continued oligomerization in the second product-determining step than in the first – in line with our experimental observations. One possible explanation for this phenomenon is rooted in better radical polarity matching after incorporation of the second BCP unit [37,38]. That is, the carbon-

Table 2: Effect of [1.1.1]propellane (**1**) equivalents relative to $\text{CF}_3\text{SF}_4\text{Cl}$ on selectivity.^a

entry	1 (equiv)	5 (% yield) ^b	3 (% yield) ^b	5:3
1	1.0	80%	10%	7.7:1.0
2	2.0	71%	21%	3.4:1.0
3	3.0	65%	31%	2.1:1.0
4	4.0	55%	40%	1.4:1.0
5	6.0	49%	40%	1.2:1.0
6	8.0	39%	46%	1.0:1.2
7	10	33%	62%	1.0:1.9
8	20	31%	65%	1.0:2.1
9 ^c	6.0	35%	60% (53%)^d	1.0:1.7

^aA 0.1 M solution of $\text{CF}_3\text{SF}_4\text{Cl}$ in *n*-pentane (0.03 mmol) was added to a 0.8 M solution of [1.1.1]propellane in Et_2O under Ar atmosphere and stirred at rt for 3 h. ^bYield determined by ^{19}F NMR. ^c $\text{CF}_3\text{SF}_4\text{Cl}$ was added portion-wise. ^dIsolated yield.

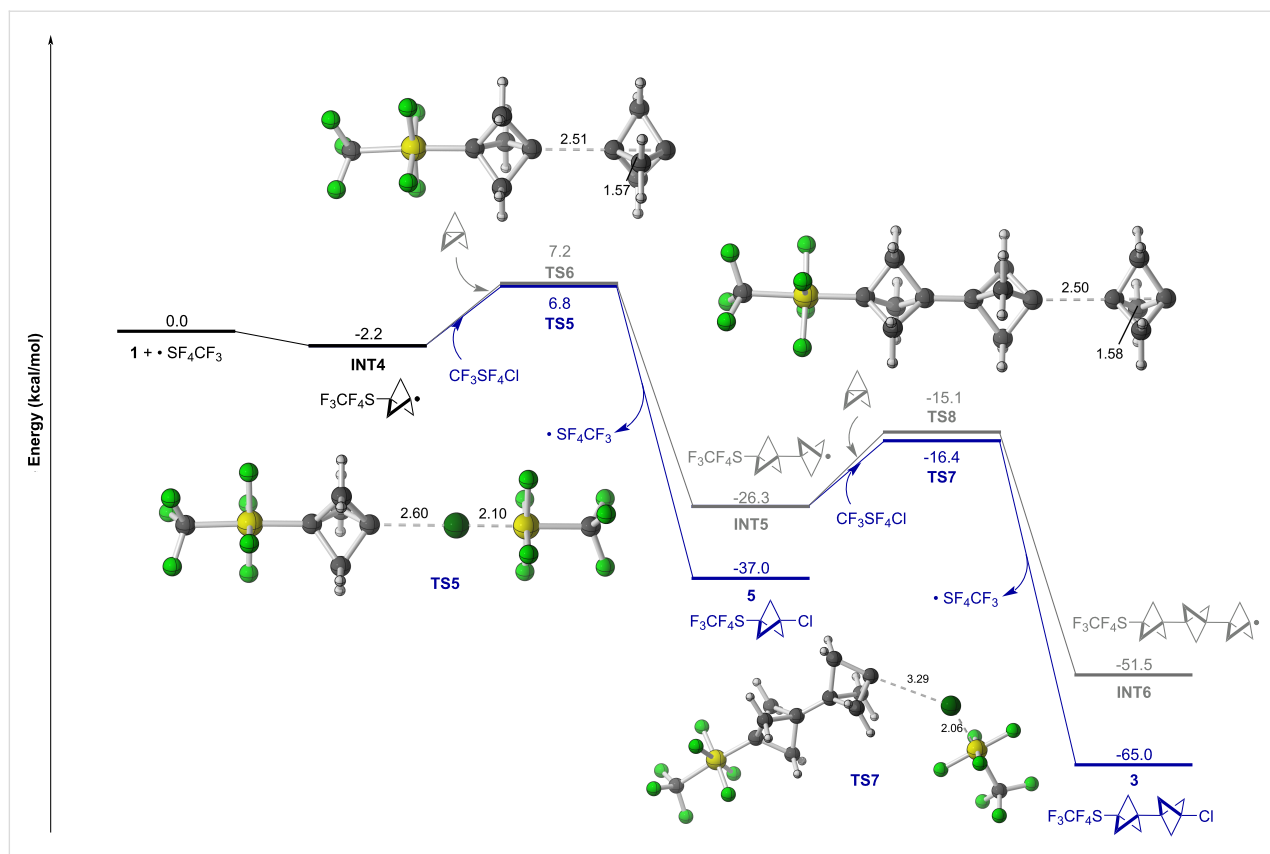


Figure 3: Computed free energy profile for the oligomerization of [1.1.1]propellane (**1**) following CF_3SF_4 radical addition at the PW-PB95-D4/def2-QZVPP//PCM(Et_2O)- ω B97X-D/def2-TZVP level of theory.

centered radicals in both **INT1** and **INT4** are closer to strong electron-withdrawing groups than are the radical centers in **INT2** and **INT5**, rendering **INT1** and **INT4** relatively more electrophilic. Inductive effects drop off steeply with distance, and it is also established that a substituent (or, e.g., a radical or cation) on the transannular carbon atom of a bicyclopentyl moiety can interact through space [35,63,64]. The consequence is ostensibly that more "nucleophilic" **INT2** and **INT5** are better matched for Cl atom abstraction from the "electrophilic" reagent (SF_5Cl or $\text{CF}_3\text{SF}_4\text{Cl}$).

To test this hypothesis, we examined computed trends in various electronic parameters for the **INT1–INT3** and the **INT4–INT6** series (Table 3). For instance, across several charge models (i.e., Hirshfeld [65], NPA [66–68], and CHELPG [69]), the charge (q) on the carbon atom on which the radical is centered becomes more negative (or less positive) the farther it is from either the SF_5 or CF_3SF_4 substituent, consistent with the notion that it becomes more nucleophilic. Moreover, the Δq is largest between the first two intermediates in both series – **INT1** vs **INT2** and **INT3** vs **INT4** – indicating that the most dramatic change in bicyclopentyl radical philicity would arise after incorporation of the second BCP unit.

In addition to charge models, we evaluated global reactivity indices (ω : electrophilicity index [70] and N : nucleophilicity index [71]) within the conceptual density functional theory (CDFT) framework [72–74]. The data show that BCP has a higher N value – thus stronger nucleophilic tendency – compared to both SF_5Cl and $\text{CF}_3\text{SF}_4\text{Cl}$. Conversely, comparison of ω values shows significantly higher electrophilicity of SF_5Cl and $\text{CF}_3\text{SF}_4\text{Cl}$ compared to BCP. These results, coupled with decreasing ω and increasing N when more BCP units are incorporated, lend qualitative support to our radical polarity matching hypothesis. Moreover, assessment of radical Fukui functions (f^0) [75] indicates that both SF_5Cl and $\text{CF}_3\text{SF}_4\text{Cl}$ are intrinsically more susceptible to radical attack than **1**, which is consistent with the lower computed barriers for Cl atom abstraction in each case.

These computed trends also potentially account for the fact that selectivity for the [2]stiffane (i.e., truncated oligomerization) using aryl- SF_4Cl reagents was not observed. On the basis of CDFT results, a model aryl- SF_4Cl compound (i.e., 5-chloropyrimidyl- SF_4Cl) was determined to be significantly less "electrophilic" than SF_5Cl or $\text{CF}_3\text{SF}_4\text{Cl}$, consistent with a reduction in the radical polarity matching effect (see Supporting Informa-

Table 3: Key indices computed to compare reactivity. Partial charges (q) and condensed Fukui functions are evaluated at the reacting carbon or chlorine atom and are in units of elementary charge (e).^a

compound	q(Hirshfeld) (e)	q(NPA) (e)	q(CHELPG) (e)	f^0 (e) ^b	ω (eV) ^c	N (eV) ^d
1	-0.090	-0.069	-0.255	0.235	0.82	1.70
SF ₅ Cl	-0.055	-0.160	0.030	0.534	2.48	-0.74
CF ₃ SF ₄ Cl	-0.061	-0.150	0.056	0.527	2.52	-0.66
INT1	-0.019	0.092	-0.125	0.307	2.70	2.95
INT2	-0.053	0.073	-0.196	0.347	1.78	3.58
INT3	-0.060	0.065	-0.214	0.345	1.66	3.77
INT4	-0.019	0.092	-0.144	0.301	2.74	2.97
INT5	-0.053	0.073	-0.193	0.346	1.78	3.59
INT6	-0.060	0.064	-0.214	0.345	1.65	3.77

^aCalculations performed at the PCM(Et₂O)-ωB97X-D/def2-TZVP level of theory. ^bRadical Fukui function. ^cElectrophilicity index. ^dNucleophilicity index.

tion File 1 for details). This was difficult to predict or rationalize based on calculation of free energies of activation alone. Overall, our results suggest that this alternating polarity matching effect is subtle and subject to mitigation yet can lead to desirable products if employed thoughtfully.

Lastly, following our synthetic and computational studies, accessing a CF₃SF₄-containing [2]staffane in good yield and for the first time created an opportunity for structural analysis. We previously reported and contextualized single-crystal X-ray diffraction (SC-XRD) data on **2** [36]; thus, we proceeded to grow crystals of **3** suitable for X-ray analysis through slow evaporation of ethyl acetate.

To our surprise, an initial measurement of **3** at 90 K revealed an unusually large unit cell ($a = 7.14 \text{ \AA}$, $b = 21.38 \text{ \AA}$, and $c = 44.04 \text{ \AA}$). Following structure solution and refinement [76], we found that **3** crystallizes in an orthorhombic space group $P2_12_12_1$ with five symmetry independent moieties ($Z' = 5$) and with no solvent present in the unit cell as an inversion twin (Figure 4). After close examination of the model, we noticed that the c -axis was roughly divisible by five with a substructure of $Z' = 1$. This suggested that the $Z' = 5$ unit cell may be due to a phase transition caused by anisotropic contraction [77].

In fact, we confirmed that a phase transition had occurred following structure determination at 240 K [78,79]. The X-ray data revealed that **3** crystallizes in the centrosymmetric orthorhombic space group $Pnma$ in the high temperature phase (HTP) with cell axes $a = 21.56 \text{ \AA}$, $b = 8.95 \text{ \AA}$, and $c = 7.28 \text{ \AA}$, in contrast to $P2_12_12_1$ in the low temperature phase (LTP). Note that the b -axis is roughly 1/5 of the c -axis observed at 90 K (the axial rearrangement is due to the change in space group). To discern the approximate temperature of the phase transition, the unit cell was measured in 20 K increments upon cooling from 260 K down to 100 K; additional details are reported in Supporting Information File 1. Interestingly, the original LTP unit cell was not detected; instead, only the reduced cell observed in the HTP was found at all temperatures. However, after warming the same crystal of **3** back to room temperature, it was rapidly cooled to 100 K under a stream of N₂ and the larger, disordered cell was observed once more [80]. (These observations also prompted us to measure a structure of **2** at 240 K; in this case, the unit cell is virtually identical at both high and low temperatures, indicating no phase transition had occurred – see Supporting Information File 1 for details.)

Accordingly, we gather that the rate of cooling plays an important role whereby rapid cooling effectively "shocks" the crystal

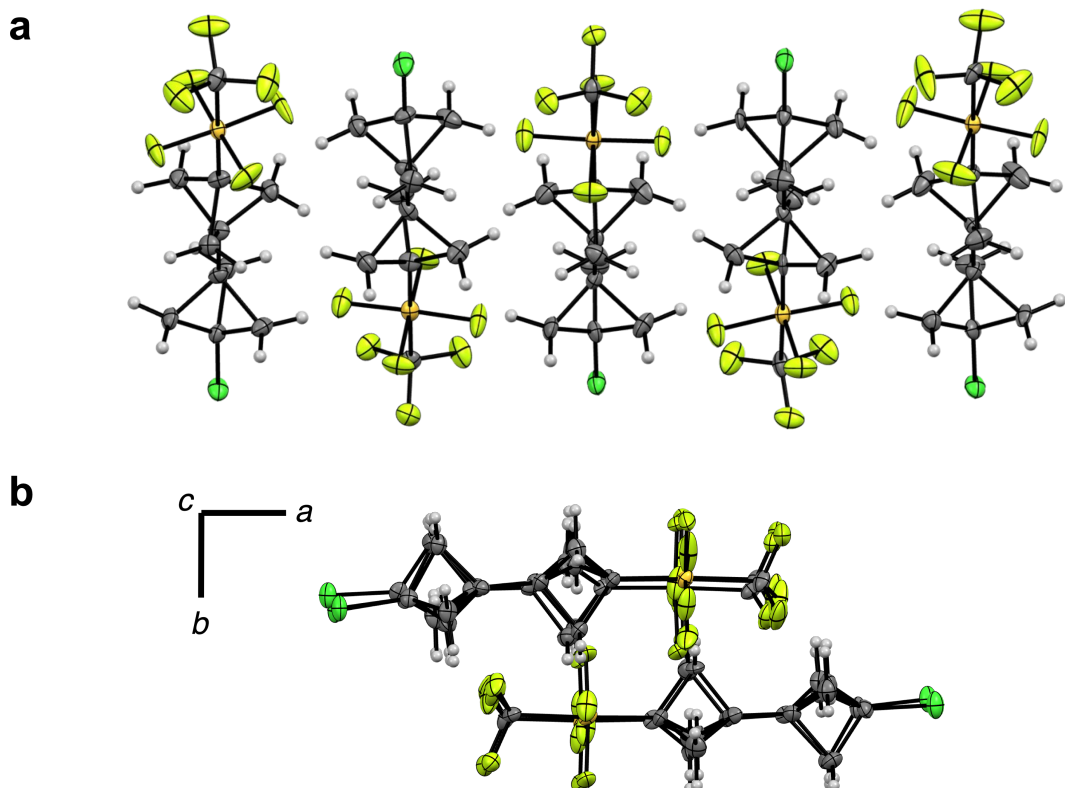


Figure 4: (A) The molecular structure of **3** at 90 K with 5 independent moieties in the asymmetric axis viewed along the *b*-axis. (B) The asymmetric unit of **3** at 90 K viewed along the *c*-axis. Thermal displacement ellipsoids depicted at 50% probability.

of **3**, compressing the unit cell isotropically, and ultimately leads to more disorder in the asymmetric unit [81]. This unexpected observation suggests that CF_3SF_4 -containing [2]staffanes, in particular, warrant additional studies and may be of interest, e.g., in liquid crystal design.

Conclusion

Suppressing $[n]$ staffane formation beyond $n = 1$ in radical chain reactions involving [1.1.1]propellane (**1**) tends to be more manageable than controlling oligomerization. However, under the right circumstances, alternating radical polarity matching throughout the chain propagation steps could be one way to theoretically "switch off" oligomerization beyond formation of a [2]staffane. Using this logic, our synthetic and computational study demonstrates that selective one-pot syntheses of [2]staffanes can be achieved when employing reagents that serve as radical sources of "extreme" electron-withdrawing groups (e.g., SF_5 or CF_3SF_4), which impact relative philicities of the bicyclopentyl radical intermediates. Over the course of this study, we also found that the SF_5 - and CF_3SF_4 -containing [2]staffanes reported herein are structurally interesting in their own right. Future work will examine potential applications of **2** and **3** and explore tactics for C–Cl bond functionalization.

Supporting Information

Supporting Information File 1

Experimental procedures, characterization data, NMR spectra, computational details, and X-ray crystallographic experimental details.

[<https://www.beilstein-journals.org/bjoc/content/supplementary/1860-5397-20-259-S1.pdf>]

Supporting Information File 2

LTP X-ray crystal structure of compound **3** (2357079.cif), HTP X-ray crystal structure of compound **3** (2357080.cif) and X-ray crystal structure of compound **2** at 240 K (238115.cif).

[<https://www.beilstein-journals.org/bjoc/content/supplementary/1860-5397-20-259-S2.zip>]

Acknowledgements

C.R.P. and Y.K. thank Dr. Nils Trapp (ETH Zürich) for helpful discussions. The authors also thank the UC Davis core NMR facility.

Funding

C.R.P. thanks the NIH/NIGMS (R35GM150861) and the University of California, Davis for financial support. W.Y.K. thanks the Croucher Foundation for financial support through a doctoral scholarship. W.Y.K. and D.J.T. thank the NSF ACCESS program (CHE030089) for computational support. The authors also thank the NSF (CHE1531193) for the Dual Source X-ray Diffractometer.

ORCID® IDs

Jón Atiba Buldt - <https://orcid.org/0009-0005-4900-0479>
 Wang-Yeuk Kong - <https://orcid.org/0000-0002-4592-0666>
 Yannick Kraemer - <https://orcid.org/0000-0002-2136-7253>
 Ansh Hiten Patel - <https://orcid.org/0009-0006-2278-9227>
 James C. Fettinger - <https://orcid.org/0000-0002-6428-4909>
 Dean J. Tantillo - <https://orcid.org/0000-0002-2992-8844>
 Cody Ross Pitts - <https://orcid.org/0000-0003-1047-8924>

Data Availability Statement

All experimental data that supports the findings of this study are available in the published article and/or the supporting information to this article; coordinates for computed structures are openly available in ioChem-BD at <https://doi.org/10.19061/iochem-bd-6-384>.

References

- Shire, B. R.; Anderson, E. A. *JACS Au* **2023**, *3*, 1539–1553. doi:10.1021/jacsau.3c00014
- Kaszynski, P.; Friedli, A. C.; Michl, J. *J. Am. Chem. Soc.* **1992**, *114*, 601–620. doi:10.1021/ja00028a029
- Levin, M. D.; Kaszynski, P.; Michl, J. *Chem. Rev.* **2000**, *100*, 169–234. doi:10.1021/cr990094z
- Dilmaç, A. M.; Spulig, E.; de Meijere, A.; Bräse, S. *Angew. Chem., Int. Ed.* **2017**, *56*, 5684–5718. doi:10.1002/anie.201603951
- Kaszynski, P.; Michl, J. *J. Am. Chem. Soc.* **1988**, *110*, 5225–5226. doi:10.1021/ja00223a070
- Friedli, A. C.; Lynch, V. M.; Kaszynski, P.; Michl, J. *Acta Crystallogr., Sect. A: Found. Crystallogr.* **1990**, *46*, 377–389. doi:10.1107/s0108768189014096
- Kaszynski, P.; Friedli, A. C.; McMurdie, N. D.; Michl, J. *Mol. Cryst. Liq. Cryst. (1969-1991)* **1990**, *191*, 193–197. doi:10.1080/00268949008038593
- Friberg, S. E.; Kayali, I.; Kaszynski, P.; Michl, J. *Langmuir* **1992**, *8*, 996–998. doi:10.1021/la00039a041
- Janecki, T.; Shi, S.; Kaszynski, P.; Michl, J. *Collect. Czech. Chem. Commun.* **1993**, *58*, 89–104. doi:10.1135/cccc19930089
- Messner, M.; Kozhushkov, S. I.; de Meijere, A. *Eur. J. Org. Chem.* **2000**, 1137–1155. doi:10.1002/1099-0690(200004)2000:7<1137::aid-ejoc1137>3.0.co;2-2
- Zimmerman, H. E.; Goldman, T. D.; Hirzel, T. K.; Schmidt, S. P. *J. Org. Chem.* **1980**, *45*, 3933–3951. doi:10.1021/jo01308a001
- Obeng, Y. S.; Laing, M. E.; Friedli, A. C.; Yang, H. C.; Wang, D.; Thulstrup, E. W.; Bard, A. J.; Michl, J. *J. Am. Chem. Soc.* **1992**, *114*, 9943–9952. doi:10.1021/ja00051a029
- Joran, A. D.; Leland, B. A.; Geller, G. G.; Hopfield, J. J.; Dervan, P. B. *J. Am. Chem. Soc.* **1984**, *106*, 6090–6092. doi:10.1021/ja00332a062
- Leland, B. A.; Joran, A. D.; Felker, P. M.; Hopfield, J. J.; Zewail, A. H.; Dervan, P. B. *J. Phys. Chem.* **1985**, *89*, 5571–5573. doi:10.1021/j100272a002
- Murthy, G. S.; Hassenrück, K.; Lynch, V. M.; Michl, J. *J. Am. Chem. Soc.* **1989**, *111*, 7262–7264. doi:10.1021/ja00200a057
- Yang, H. C.; Magnera, T. F.; Lee, C.; Bard, A. J.; Michl, J. *Langmuir* **1992**, *8*, 2740–2746. doi:10.1021/la00047a026
- Mazières, S.; Raymond, M. K.; Raabe, G.; Prodi, A.; Michl, J. *J. Am. Chem. Soc.* **1997**, *119*, 6682–6683. doi:10.1021/ja971059h
- Lovering, F.; Bikker, J.; Humblet, C. *J. Med. Chem.* **2009**, *52*, 6752–6756. doi:10.1021/jm901241e
- Tsien, J.; Hu, C.; Merchant, R. R.; Qin, T. *Nat. Rev. Chem.* **2024**, *8*, 605–627. doi:10.1038/s41570-024-00623-0
- Stepan, A. F.; Subramanyam, C.; Efremov, I. V.; Dutra, J. K.; O'Sullivan, T. J.; DiRico, K. J.; McDonald, W. S.; Won, A.; Dorff, P. H.; Nolan, C. E.; Becker, S. L.; Pustilnik, L. R.; Riddell, D. R.; Kauffman, G. W.; Kormos, B. L.; Zhang, L.; Lu, Y.; Capetta, S. H.; Green, M. E.; Karki, K.; Sibley, E.; Atchison, K. P.; Hallgren, A. J.; Oborski, C. E.; Robshaw, A. E.; Sneed, B.; O'Donnell, C. J. *J. Med. Chem.* **2012**, *55*, 3414–3424. doi:10.1021/jm300094u
- Locke, G. M.; Bernhard, S. S. R.; Senge, M. O. *Chem. – Eur. J.* **2019**, *25*, 4590–4647. doi:10.1002/chem.201804225
- Mykhailiuk, P. K. *Org. Biomol. Chem.* **2019**, *17*, 2839–2849. doi:10.1039/c8ob02812e
- Tse, E. G.; Houston, S. D.; Williams, C. M.; Savage, G. P.; Rendina, L. M.; Hallyburton, I.; Anderson, M.; Sharma, R.; Walker, G. S.; Obach, R. S.; Todd, M. H. *J. Med. Chem.* **2020**, *63*, 11585–11601. doi:10.1021/acs.jmedchem.0c00746
- Cuadros, S.; Goti, G.; Barison, G.; Raulli, A.; Bortolato, T.; Pelosi, G.; Costa, P.; Dell'Amico, L. *Angew. Chem., Int. Ed.* **2023**, *62*, e202303585. doi:10.1002/anie.202303585
- Rehm, J. D. D.; Zierner, B.; Szeimies, G. *Eur. J. Org. Chem.* **2001**, 1049–1052. doi:10.1002/1099-0690(200103)2001:6<1049::aid-ejoc1049>3.0.co;2-v
- Mazal, C.; Paraskos, A. J.; Michl, J. *J. Org. Chem.* **1998**, *63*, 2116–2119. doi:10.1021/jo971419j
- Bunz, U.; Szeimies, G. *Tetrahedron Lett.* **1990**, *31*, 651–652. doi:10.1016/s0040-4039(09)94592-1
- Blokhin, A. V.; Tyurekhodzhaeva, M. A.; Sadovaya, N. K.; Zefirov, N. S. *Russ. Chem. Bull.* **1989**, *38*, 1779. doi:10.1007/bf00956980
- Sadovaya, N. K.; Blokhin, A. V.; Tyurekhodzhaeva, M. A.; Grishin, Y. K.; Surmina, L. S.; Koz'min, A. S.; Zefirov, N. S. *Russ. Chem. Bull.* **1990**, *39*, 637–638. doi:10.1007/bf00959608
- Cheng, X.-Y.; Du, F.-S.; Li, Z.-C. *J. Polym. Sci. (Hoboken, NJ, U. S.)* **2023**, *61*, 472–481. doi:10.1002/pol.20220635
- Bunz, U.; Szeimies, G. *Tetrahedron Lett.* **1989**, *30*, 2087–2088. doi:10.1016/s0040-4039(01)93718-9
- Bunz, U.; Polborn, K.; Wagner, H.-U.; Szeimies, G. *Chem. Ber.* **1988**, *121*, 1785–1790. doi:10.1002/cber.19881211014
- Sadovaya, N. K.; Blokhin, A. V.; Surmina, L. S.; Tyurekhodzhaeva, M. A.; Koz'min, A. S.; Zefirov, N. S. *Russ. Chem. Bull.* **1990**, *39*, 2224. doi:10.1007/bf01557749
- Wiberg, K. B.; Waddell, S. T. *J. Am. Chem. Soc.* **1990**, *112*, 2194–2216. doi:10.1021/ja00162a022
- Friedli, A. C.; Kaszynski, P.; Michl, J. *Tetrahedron Lett.* **1989**, *30*, 455–458. doi:10.1016/s0040-4039(00)95226-2

36. Kraemer, Y.; Ghiazza, C.; Ragan, A. N.; Ni, S.; Lutz, S.; Neumann, E. K.; Fettinger, J. C.; Nöthling, N.; Goddard, R.; Cornell, J.; Pitts, C. R. *Angew. Chem., Int. Ed.* **2022**, *61*, e202211892. doi:10.1002/anie.202211892
37. Shou, J.-Y.; Xu, X.-H.; Qing, F.-L. *Angew. Chem., Int. Ed.* **2021**, *60*, 15271–15275. doi:10.1002/anie.202103606
38. Pitts, C. R.; Santschi, N.; Togni, A. Method For Preparing a Polyfluorinated Compound. WO Patent WO/2019/229103, Dec 5, 2019.
39. Pitts, C. R.; Bornemann, D.; Liebing, P.; Santschi, N.; Togni, A. *Angew. Chem., Int. Ed.* **2019**, *58*, 1950–1954. doi:10.1002/anie.201812356
40. Häfliger, J.; Pitts, C. R.; Bornemann, D.; Käser, R.; Santschi, N.; Charpentier, J.; Otth, E.; Trapp, N.; Verel, R.; Lüthi, H. P.; Togni, A. *Chem. Sci.* **2019**, *10*, 7251–7259. doi:10.1039/c9sc02162k
41. Bornemann, D.; Pitts, C. R.; Ziegler, C. J.; Pietrasik, E.; Trapp, N.; Kueng, S.; Santschi, N.; Togni, A. *Angew. Chem., Int. Ed.* **2019**, *58*, 12604–12608. doi:10.1002/anie.201907359
42. Brüning, F.; Pitts, C. R.; Kalim, J.; Bornemann, D.; Ghiazza, C.; de Montmollin, J.; Trapp, N.; Billard, T.; Togni, A. *Angew. Chem., Int. Ed.* **2019**, *58*, 18937–18941. doi:10.1002/anie.201910594
43. Ragan, A. N.; Kraemer, Y.; Kong, W.-Y.; Prasad, S.; Tantillo, D. J.; Pitts, C. R. *Angew. Chem., Int. Ed.* **2022**, *61*, e202208046. doi:10.1002/anie.202208046
44. Kraemer, Y.; Bergman, E. N.; Togni, A.; Pitts, C. R. *Angew. Chem., Int. Ed.* **2022**, *61*, e202205088. doi:10.1002/anie.202205088
45. Tyurekhodzhaeva, M. A.; Bratkova, A. A.; Blokhin, A. V.; Brel, V. K.; Koz'min, A. S.; Zefirov, N. S. *J. Fluorine Chem.* **1991**, *55*, 237–240. doi:10.1016/s0022-1139(00)82351-9
46. De Vleeschouwer, F.; Van Speybroeck, V.; Waroquier, M.; Geerlings, P.; De Proft, F. *Org. Lett.* **2007**, *9*, 2721–2724. doi:10.1021/o1071038k
47. Domingo, L. R.; Pérez, P. *Org. Biomol. Chem.* **2013**, *11*, 4350–4358. doi:10.1039/c3ob40337h
48. Kraemer, Y.; Buldt, J. A.; Kong, W.-Y.; Stephens, A. M.; Ragan, A. N.; Park, S.; Haidar, Z. C.; Patel, A. H.; Shey, R.; Dagan, R.; McLoughlin, C. P.; Fettinger, J. C.; Tantillo, D. J.; Pitts, C. R. *Angew. Chem., Int. Ed.* **2024**, *63*, e202319930. doi:10.1002/anie.202319930
49. Zhao, X.; Shou, J.-Y.; Qing, F.-L. *Sci. China: Chem.* **2023**, *66*, 2871–2877. doi:10.1007/s11426-023-1715-2
50. Nguyen, T. M.; Popek, L.; Matchavariani, D.; Blanchard, N.; Bizet, V.; Cahard, D. *Org. Lett.* **2024**, *26*, 365–369. doi:10.1021/acs.orglett.3c04043
51. Goerigk, L.; Grimme, S. *J. Chem. Theory Comput.* **2011**, *7*, 291–309. doi:10.1021/ct100466k
52. Caldeweyher, E.; Bannwarth, C.; Grimme, S. *J. Chem. Phys.* **2017**, *147*, 034112. doi:10.1063/1.4993215
53. Caldeweyher, E.; Ehlert, S.; Hansen, A.; Neugebauer, H.; Spicher, S.; Bannwarth, C.; Grimme, S. *J. Chem. Phys.* **2019**, *150*, 154122. doi:10.1063/1.5090222
54. Weigend, F.; Ahlrichs, R. *Phys. Chem. Chem. Phys.* **2005**, *7*, 3297–3305. doi:10.1039/b508541a
55. Cancès, E.; Mennucci, B.; Tomasi, J. *J. Chem. Phys.* **1997**, *107*, 3032–3041. doi:10.1063/1.474659
56. Chai, J.-D.; Head-Gordon, M. *Phys. Chem. Chem. Phys.* **2008**, *10*, 6615–6620. doi:10.1039/b810189b
57. Neese, F. *Wiley Interdiscip. Rev.: Comput. Mol. Sci.* **2022**, *12*, e1606. doi:10.1002/wcms.1606
58. Gaussian 16, Revision. C.01; Gaussian, Inc.: Wallingford, CT, 2016.
59. Ikeda, A.; Zhong, L.; Savoie, P. R.; von Hahmann, C. N.; Zheng, W.; Welch, J. T. *Eur. J. Org. Chem.* **2018**, 772–780. doi:10.1002/ejoc.201701568
60. Ikeda, A.; Capellan, A.; Welch, J. T. *Org. Biomol. Chem.* **2019**, *17*, 8079–8082. doi:10.1039/c9ob01797f
61. Deng, M.; Wilde, M.; Welch, J. T. *J. Org. Chem.* **2023**, *88*, 11363–11366. doi:10.1021/acs.joc.3c01177
62. Zhao, X.; Shou, J.-Y.; Newton, J. J.; Qing, F.-L. *Org. Lett.* **2022**, *24*, 8412–8416. doi:10.1021/acs.orglett.2c03540
63. Wu, J. I.-C.; Schleyer, P. v. R. *Pure Appl. Chem.* **2013**, *85*, 921–940. doi:10.1351/pac-con-13-01-03
64. Sterling, A. J.; Smith, R. C.; Anderson, E. A.; Duarte, F. J. *Org. Chem.* **2024**, *89*, 9979–9989. doi:10.1021/acs.joc.4c00857
65. Hirshfeld, F. L. *Theor. Chim. Acta* **1977**, *44*, 129–138. doi:10.1007/bf00549096
66. Reed, A. E.; Weinstock, R. B.; Weinhold, F. J. *Chem. Phys.* **1985**, *83*, 735–746. doi:10.1063/1.449486
67. NBO 7.0; Theoretical Chemistry Institute, University of Wisconsin: Madison, WI, USA, 2018.
68. Glendening, E. D.; Landis, C. R.; Weinhold, F. J. *Comput. Chem.* **2019**, *40*, 2234–2241. doi:10.1002/jcc.25873
69. Breneman, C. M.; Wiberg, K. B. *J. Comput. Chem.* **1990**, *11*, 361–373. doi:10.1002/jcc.540110311
70. Parr, R. G.; Szentpály, L. v.; Liu, S. *J. Am. Chem. Soc.* **1999**, *121*, 1922–1924. doi:10.1021/ja983494x
71. Domingo, L. R.; Chamorro, E.; Pérez, P. *J. Org. Chem.* **2008**, *73*, 4615–4624. doi:10.1021/jo800572a
72. Lu, T.; Chen, Q. Realization of Conceptual Density Functional Theory and Information-Theoretic Approach in Multiwfn Program. In *Conceptual Density Functional Theory*; Liu, S., Ed.; Wiley-VCH: Weinheim, Germany, 2022; Vol. 2, pp 631–647. doi:10.1002/9783527829941.ch31
73. Geerlings, P.; De Proft, F.; Langenaeker, W. *Chem. Rev.* **2003**, *103*, 1793–1874. doi:10.1021/cr990029p
74. Lu, T.; Chen, F. *J. Comput. Chem.* **2012**, *33*, 580–592. doi:10.1002/jcc.22885
75. Parr, R. G.; Yang, W. *J. Am. Chem. Soc.* **1984**, *106*, 4049–4050. doi:10.1021/ja00326a036
76. Sheldrick, G. M. *Acta Crystallogr., Sect. C: Struct. Chem.* **2015**, *71*, 3–8. doi:10.1107/s2053229614024218
77. Stephenson, G. A. *J. Pharm. Sci.* **2006**, *95*, 821–827. doi:10.1002/jps.20442
78. Chen, L.-Z.; Huang, D.-D.; Pan, Q.-J.; Ge, J.-Z. *RSC Adv.* **2015**, *5*, 13488–13494. doi:10.1039/c4ra12690d
79. Tello, M. J.; Lopez-Echarri, A.; Zubillaga, J.; Ruiz-Larrea, I.; Zuniga, F. J.; Madariaga, G.; Gomez-Cuevas, A. *J. Phys.: Condens. Matter* **1994**, *6*, 6751–6760. doi:10.1088/0953-8984/6/34/007
80. Izumov, Y. A.; Syromyatnikov, V. N. *Phase Transitions and Crystal Symmetry*; Kluwer Academic Publishers: Dordrecht, Netherlands, 1990. doi:10.1007/978-94-009-1920-4
81. Chatteraj, S.; Sun, C. C. *Crystals* **2023**, *13*, 270. doi:10.3390/crust13020270

License and Terms

This is an open access article licensed under the terms of the Beilstein-Institut Open Access License Agreement (<https://www.beilstein-journals.org/bjoc/terms>), which is identical to the Creative Commons Attribution 4.0 International License (<https://creativecommons.org/licenses/by/4.0>). The reuse of material under this license requires that the author(s), source and license are credited. Third-party material in this article could be subject to other licenses (typically indicated in the credit line), and in this case, users are required to obtain permission from the license holder to reuse the material.

The definitive version of this article is the electronic one which can be found at:

<https://doi.org/10.3762/bjoc.20.259>